THE JOURNAL OF BIOLOGICAL CHEMISTRY
Vol. 279, No. 2, Issue of January 9, pp. 1040–1049, 2004

Printed in U.S.A.

Tetrapandins, a New Class of Scorpion Toxins That Specifically Inhibit Store-operated Calcium Entry in Human Embryonic Kidney-293 Cells*

Received for publication, July 28, 2003, and in revised form, October 17, 2003
Published, JBC Papers in Press, October 28, 2003, DOI 10.1074/jbc.M308234200

Andree Shalabi‡, Fernando Zamudio§, Xiaoyan Wu‡, Andrea Scaloni¶, Lourival D. Possani§‖, and Mitchel L. Villereal‡‖**

From the ‡Department of Neurobiology, Pharmacology and Physiology, The University of Chicago, Chicago, Illinois 60637, the §Department of Molecular Medicine and Bioprocesses, Institute of Biotechnology, National Autonomous University of Mexico, Avenida Universidad, Apartado Postal 510-3, Cuernavaca 62210, Mexico, and the ¶Proteomics and Mass Spectrometry Laboratory, Istituto per il Sistema Produzione Animale in Ambiente Mediterraneo, National Research Council, via Argine 1085, Naples 80147, Italy

Venoms from 14 snakes and four scorpions were screened for inhibitory activities toward store-operated Ca^{2+} entry (SOCE) in human embryonic kidney-293 cells. An inhibitory activity was found in venom from the African scorpion *Pandinus imperator*. The active agent of this venom was purified by gel filtration and reverse-phase high pressure liquid chromatography methods. Sequence information on the purified fraction, by automatic Edman degradation and mass spectrometry analysis, identified the activity as being contained in two tetrapeptides, which we have named tetrapandins. We demonstrate that synthesized tetrapandins have inhibitory activity for SOCE in human embryonic kidney-293 cells while having no effect on either thapsigargin- or carbachol-stimulated release of Ca^{2+} stores. These toxins should be extremely useful in future studies to determine downstream events regulated by SOCE as well as to determine whether multiple pathways exist for thapsigargin-stimulated Ca^{2+} entry.

A large number of receptors utilize Ca^{2+} as a second messenger to initiate downstream physiological processes. In the case of G protein-coupled receptors, the Ca^{2+} response generally is biphasic with an initial rapid spike of Ca^{2+}, due to release of internal Ca^{2+} stores, followed by a longer, more sustained response. In some cases, the sustained response takes the form of a stable Ca^{2+} plateau, while in other cases sustained Ca^{2+} oscillations are observed; both the Ca^{2+} plateau and sustained Ca^{2+} oscillations are dependent on a continued influx of external Ca^{2+}. Generally this Ca^{2+} influx is mediated by non-voltage-gated channels (1–4), and a great deal of effort is being exerted to characterize these channels and the proteins responsible for forming these channels. There appear to be multiple types of non-voltage-gated Ca^{2+} channels stimulated by agonists of G protein-coupled receptors, one of which, the store-operated channels (SOCs),[1] mediates what was originally referred to as capacitative Ca^{2+} entry (5) but now often called store-operated Ca^{2+} entry (SOCE). These channels are activated in response to depletion of internal Ca^{2+} stores. While there are a number of plausible theories on the mechanism by which store depletion activates these channels (6, 7), there is still no complete model for this process. Likewise some progress has been made in identifying members of the TRPC channel family as the likely protein mediators of SOCE, but there is still much controversy in the literature concerning which of the TRPC family members are store-operated and which are receptor-operated. In addition, there is some question as to whether more than one subtype of SOCE might exist (8) as well as a relative dearth of information concerning the downstream consequences of SOCE.

One limitation in the characterization of SOCs and the investigation of the downstream consequences of SOCE has been the lack of an inhibitor with high affinity and high specificity for SOCs. While a number of substances have been used to inhibit SOCE, these agents in general lack the specificity required to fully characterize these channels and to determine unequivocally which downstream physiological events are regulated by Ca^{2+} entering via SOCs. For example, SKF96365 has frequently been used to inhibit SOCE and to investigate events regulated downstream of SOCE (9). However, SKF96365 has been demonstrated to inhibit Na^+ channels (10), K^+ channels (11), and maitotoxin-induced Ca^{2+} entry (12, 13) and to facilitate nicotinic receptor desensitization (14). Other agents utilized as inhibitors of SOCs, such as carboxyamidotriazole (15) and 2-aminoethoxydiphenyl borate (2-APB) (16), have also been demonstrated to have inhibitory effects on other channels and transport molecules with carboxyamidotriazole being reported as an inhibitor of voltage-gated Ca^{2+} channels (17) and 2-APB being reported to inhibit $InsP_3$-mediated Ca^{2+} release (18–20), K^+ currents (21), sarcoplasmic reticulum Ca^{2+}-ATPase (22), gap junctions (23), and Ca^{2+}-induced Ca^{2+} release from isolated mitochondria (24) and even to activate a novel calcium-permeable cation channel (25). Given all of the

* This work was supported by National Council of Science and Technology (CONACyT), Mexican Government, Grants Z-005 and 40251-Q (to L. D. P.) and by NIGMS, National Institutes of Health Grant GM-54500 (to M. L. V.). The costs of publication of this article were defrayed in part by the payment of page charges. This article must therefore be hereby marked "*advertisement*" in accordance with 18 U.S.C. Section 1734 solely to indicate this fact.

‖ The Possani and Villereal laboratories made equal contributions to this work.

** To whom correspondence should be addressed: Dept. of Neurobiology, Pharmacology and Physiology, The University of Chicago, 947 E. 58th St., Chicago, IL 60637. E-mail: mitch@drugs.bsd.uchicago.edu.

[1] The abbreviations used are: SOC, store-operated channel; SOCE, store-operated Ca^{2+} entry; HEK, human embryonic kidney; HPLC, high pressure liquid chromatography; TRPC, transient receptor potential channel; 2-APB, 2-aminoethoxydiphenyl borate; $InsP_3$, inositol 1,4,5-trisphosphate; AM, acetoxymethyl ester; HBSS, Hanks' balanced salt solution; OAG, 1-oleolyl-2-acetyl-*sn*-glycerol; MALDI-TOF, matrix-assisted laser desorption ionization time-of-flight; MS, mass spectrometry; CCh, carbachol.

side effects of existing inhibitors of SOCs, there is a clear need for a potent, specific inhibitor of SOCE.

One fertile source of ion channel inhibitors has been the venom of poisonous snakes, scorpions, spiders, and sea snails. Peptide toxins have been purified from complex venoms that block Na^+ channels (26), K^+ channels (27), voltage-gated Ca^{2+} channels (28), and receptor-operated channels such as the *N*-methyl-D-aspartate receptor (29). From the utilization of these peptide toxins, much has been learned about the subunit composition of these channels, their mode of activation and inactivation, and the downstream events regulated by ion movements through these channels. To date, toxins for non-voltage-gated channels such as SOCs have not been identified. Clearly the discovery of a peptide toxin specific for SOCs would allow a level of study of these channels that has not been possible with current inhibitors. In this report, we describe our search for a peptide toxin in venoms of snakes and scorpions, the purification of the toxin from the *Pandinus imperator* scorpion venom, the identification of the toxin sequence, and the synthesis and functional effect of the peptide toxins we have named tetrapandins. These toxins should be extremely useful in future studies to determine downstream events regulated by SOCE as well to determine whether multiple pathways exist for thapsigargin-stimulated Ca^{2+} entry.

EXPERIMENTAL PROCEDURES

Materials—Fura-2 free acid, fura-2 AM, and Pluronic F-127 were purchased from Molecular Probes; thapsigargin was purchased from LC Laboratory. Hanks' balanced salt solution (HBSS), Ca^{2+}-free, Mg^{2+}-free, HCO_3^--free HBSS, Dulbecco's modified Eagle's medium, penicillin/streptomycin, L-glutamine, and trypsin-EDTA were purchased from Invitrogen. Chelex-100 came from Bio-Rad, and 1-oleolyl-2-acetyl-*sn*-glycerol (OAG), along with other chemicals, were purchased from Sigma.

Venom Purification Procedure—All snake species, kept alive at the Kentucky Reptile Zoo (Slade, KY), were milked manually by having them bite into a rubber membrane, which was stretched over a glass funnel. The venom was collected in a glass vial, and the harvest was immediately frozen after extraction and lyophilized within 1 week. The powdered venom from each species was dissolved in 1 ml of double distilled water and kept at −20 °C.

Scorpions of the species *P. imperator*, kept alive in the laboratory, were milked by electric stimulation, and their venom was dissolved in twice distilled water and centrifuged at 15,000 × *g* for 15 min. The supernatant was freeze-dried and kept at −20 °C until used. When required, samples of the soluble venom were loaded onto a Sephadex G-50 column (medium size, from Amersham Biosciences) and eluted with 20 mM ammonium acetate buffer, pH 4.7, following earlier published results (30). The active fraction (see below) was further separated using a semipreparative C18 reverse-phase column (Vydac, Hisperia, CA) of an HPLC system using a linear gradient from solution A (0.12% trifluoroacetic acid in water) to 60% solution B (0.10% trifluoroacetic acid in acetonitrile). The active fraction was further subjected to HPLC separation using an analytical Vydac C18 reverse-phase column eluted with the same gradient. Two pure peptides were obtained from this column and were further characterized.

Amino Acid Sequence and Mass Spectrometry Analysis—The peptides obtained from the HPLC system were sequenced using automatic Edman degradation in a ProSequencer apparatus (Beckman LF3000) following the protocol described by the manufacturer. The molecular weights of purified components were determined by means of a Finnigan LCQ^{Duo} ion trap mass spectrometer (San Jose, CA). Confirmation of sequence and molecular masses were obtained using a MALDI-TOF MS apparatus (Voyager DE-PRO, Applied Biosystems, Framingham, MA). Peptides were crystallized using the dried droplet technique and α-cyano-4-hydroxycinnamic as matrix. Postsource decay fragment ion spectra were acquired after isolation of the appropriate precursor by using timed ion selection. Fragment ions were refocused onto the detector by stepping the voltage applied to the reflectron and acquiring distinct spectral segments using an Acquiris digitizer at a digitization rate of 500 MHz. Individual spectra were superimposed by using the Data Explorer Version 4.0 software (Applied Biosystems).

Peptide Synthesis and Aggregation—The chemical synthesis of the peptides was performed by the solid phase method of Merrifield (31) using Fmoc (*N*-(9-fluorenyl)methoxycarbonyl)-derivatized amino acids. NovoSyn TGA resins (600 mg, 0.126 meq) were used for each peptide. Once the peptides were synthesized, they were detached from the resins, and the corresponding protecting groups of the residues were eliminated by means of reactive K (84% trifluoroacetic acid, 5% phenol, 5% H_2O, 5% thioanisole, 1% dithiothreitol) for 1 h. Deprotected peptides were precipitated with *t*-butyl methyl ether, washed three times with ether, redissolved in 20% acetic acid, and lyophilized as described. After synthesis, the peptides were purified by HPLC using the same conditions described for purification of the native peptides (see above). Their structures were confirmed by mass spectrometry analysis. The exact amino acid sequence for each one of the peptides was confirmed by dissolving them to a final concentration of 500 pmol/5 μl of 50% acetonitrile with 1% acetic acid and directly applying them into the Finnigan LCQ^{Duo} ion trap spectrometer using a Surveyor MS syringe pump delivery system. The eluate at 10 μl/min was split to allow only 5% of the sample to enter the nanospray source. The spray voltage was set to start at 1.7 kV, and the capillary temperature was set at 115 °C. For MS/MS experiments, the fragmentation source was operated with 25–35V of collision energy and 35–45% (arbitrary units) of normalized collision energy, and the scan was operated with wide band activated. All spectra were obtained in the positive ion mode. The data acquisition and the deconvolution of data were performed with the Xcalibur (Sequest) software. The MS/MS spectra were analyzed manually.

The synthetic peptide was dissolved in either HBSS or Ca $^{2+}$-free HBSS (pH 7.4) and then filter-sterilized. The sterile peptide solutions were either used directly, or they were mixed for 2 days at room temperature on a Glas-Col rotator (Fisher) and then used for calcium imaging experiments.

Cell Culture—HEK-293 cells were cultured in Dulbecco's modified Eagle's medium supplemented with 10% fetal bovine serum, 50 units/ml penicillin, 50 μg/ml streptomycin, and 2 mM glutamine. Cells were grown in an incubator at 37 °C with humidified 5% CO_2 and 95% air.

Ca^{2+} Imaging—The intracellular Ca^{2+} concentration ($[Ca^{2+}]_i$) was measured in cells loaded with the fluorescent indicator fura-2. Cells were plated onto 25-mm coverslips 1 day before the experiment. On the next morning, cells were washed twice with HEPES-buffered HBSS, loaded for 30 min with 5 μM fura-2 AM that was dissolved in HBSS supplemented with 1 mg/ml bovine serum albumin + 0.025% Pluronic F-127, and then unloaded in HBSS for another 30 min. The coverslips were mounted as the bottom of a chamber that was placed on the stage of a Nikon Diaphot inverted epifluorescence microscope equipped with a Fluor 10× objective. Cells in the chamber were perfused via an eight-channel syringe system. A suction pipette maintained a constant volume of solution (~0.5 ml) in the chamber.

An InCyt IM2™ fluorescence imaging system (dual wavelength fluorescence imaging system, Intracellular Imaging Inc., Cincinnati, OH) was used to measure $[Ca^{2+}]_i$ during the experiment. Excitation light from a xenon light source was alternately passed through 340 and 380 narrow pass filters mounted in a Sutter filter wheel (Lamda 10-C). The 510 nm emissions were captured by a cooled CCD camera (Cohu 4915). The images were transmitted to a computer and processed with the imaging software InCyt IM2™ Version 4.6. $[Ca^{2+}]_i$ was calculated by measuring the ratio of the two emission intensities for excitation at 340 and 380 nm. Calcium standard solutions, which were prepared with fura-2 potassium salt, were used to create a graph of fluorescence ratio (F_{340}/F_{380}) as a function of Ca^{2+} concentration (nM). This graph was then used to convert fluorescence ratios in an experiment to calcium concentrations. In experiments in which Ba^{2+} influx was measured, the data are reported as the ratio (F_{340}/F_{380}) since the Ba^{2+} calibrations curves for fura-2 differ from the calibration curve for Ca^{2+}.

During the experiment, an averaged response of ~800 cells from a single field on each coverslip was represented as one trace. For initial experiments, intracellular Ca^{2+} stores were depleted in the presence of extracellular Ca^{2+}, and the effect of the toxin was monitored by measuring the amount of reduction of the Ca^{2+} plateau. In later experiments where Ba^{2+} entry was monitored as a measure of the level of SOCE, the thapsigargin-stimulated Ba^{2+} entry was obtained by subtracting the slope of the Ba^{2+} leak (before stimulation) from the slope of Ba^{2+} influx (after stimulation) for each coverslip.

Nominally Ca^{2+}-free HBSS was prepared by stirring Ca^{2+}-free, Mg^{2+}-free, and HCO_3^--free HBSS with Chelex-100 beads. After filtering out the Chelex-100 beads, $MgCl_2$ was added to a final concentration of 1 mM.

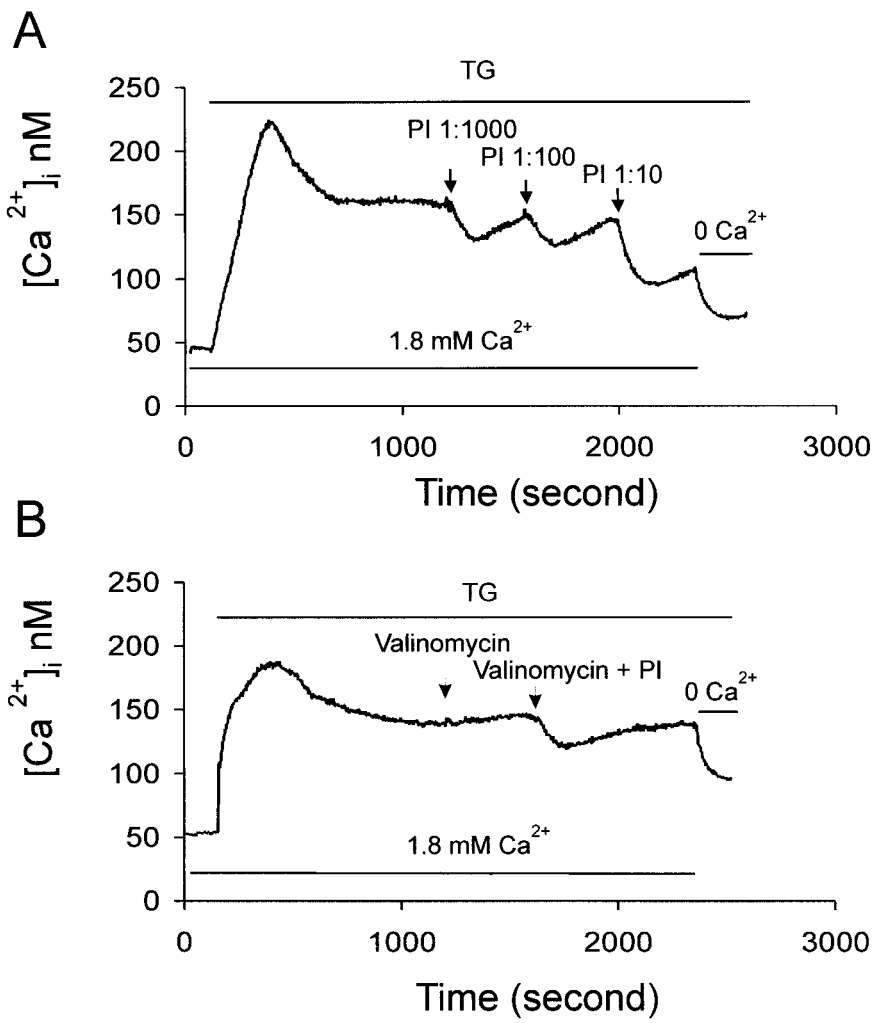

FIG. 1. **Inhibition of thapsigargin-stimulated Ca^{2+} entry by *P. imperator* scorpion venom.** Venom was collected from the African scorpion *P. imperator*, and a series of dilutions were made in HBSS. HEK-293 cells were perfused with HBSS, and the $[Ca^{2+}]_i$ was monitored by fura-2 imaging. After the establishment of a base line, cells were stimulated with thapsigargin (*TG*, 1 μM). Once the stable calcium plateau levels were reached, a series of different *P. imperator* (*PI*) venom dilutions were added (*A*). Similar fura-2 imaging experiments were performed with 10 μM valinomycin being applied shortly before and along with the venom (*B*).

RESULTS

Our initial step was to screen a variety of snake and scorpion venoms in search of an inhibitory effect on SOCE in HEK-293 cells. This was done by investigating the effect of the various venoms on thapsigargin-stimulated Ca^{2+} entry. HEK-293 cells were stimulated with 1 μM thapsigargin in the presence of HBSS. After an initial peak of Ca^{2+}, the cells establish a stable Ca^{2+} plateau phase that is rapidly dissipated upon the removal of external Ca^{2+}, indicating that the plateau is strictly dependent on continued influx of external Ca^{2+}. Various dilutions of snake and scorpion venoms were added during the Ca^{2+} plateau phase to test whether an inhibition of Ca^{2+} entry occurred. We screened a total of 14 snakes (*Agkistrodon contortrix contortrix*, *Agkistrodon contortrix mokeson*, *Crotalus durissus culminatus*, *Crotalus durissus cumanensis*, *Crotalus durissus terrificus*, *Daboia russelli russelli*, *Ophiophagus hannah*, *Naja haje*, *Naja kaouthia*, *Naja naja*, *Naja nivea*, *Naja pallida*, *Naja sputatrix*, and *Bothrops jararaca*) and four scorpion (*Hadrurus gertschi*, *Centruroides limpidus limpidus*, *Centruroides noxius*, and *P. imperator*) venoms and found effects from only one snake venom and one scorpion venom. We undertook an in-depth investigation of the inhibitory agent present in the scorpion venom. The effects of various dilutions of the venom from the African scorpion *P. imperator* are shown in Fig. 1*A*. Increasing doses of the *P. imperator* venom resulted in an enhanced inhibition of the thapsigargin-induced Ca^{2+} plateau. At this point, we were concerned that the reduction in Ca^{2+} levels might be due to membrane depolarization that resulted from inhibition or activation of some other ion channel by the venom. Although SOCs are not directly regulated by membrane depolarization, the level of SOCE can be affected by a reduction of the driving force following membrane depolarization. To determine whether this was the case, we investigated whether the addition of valinomycin, which locks the membrane in a hyperpolarized state, would eliminate the effect of the *P. imperator* venom. The data in Fig. 1*B* show that the addition of valinomycin led to a slight increase in plateau Ca^{2+} levels but did not block the effect of the *P. imperator* venom on Ca^{2+} plateau levels. We also investigated the effect of the *P. imperator* venom on thapsigargin-stimulated Ba^{2+} entry to rule out the possibility that the venom is working on Ca^{2+} extrusion mechanisms rather than on Ca^{2+} entry pathways. Since Ba^{2+} is not pumped by Ca^{2+}-ATPases (32, 33), an inhibition of Ba^{2+} entry by the venom would indicate that the effect is on a Ca^{2+} entry pathway. We observed that the venom had a significant inhibitory effect on Ba^{2+} entry (venom data not shown, but data for purified toxin shown later).

The initial step in characterization of the active agent in the *P. imperator* venom was to fractionate the venom on a gel filtration column. The Sephadex G-50 column separated several families of components based on molecular sizes (Fig. 2). Tubes corresponding to five subfractions (I–V) were pooled and lyophilized. They were all screened to determine their activity for reducing the thapsigargin-stimulated Ca^{2+} plateau levels. We observed that only fraction V from the filtration column had an effect on the thapsigargin-stimulated Ca^{2+} plateau phase. The data in Fig. 3 illustrate the effects of several doses of fraction V (*F5*) on the Ca^{2+} plateau level. We performed addi-

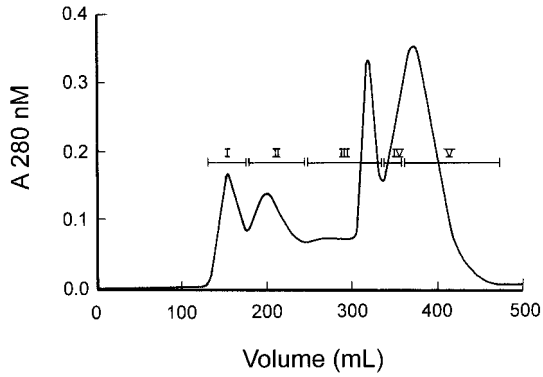

FIG. 2. **Fractionation of *P. imperator* venom by Sephadex G-50 Gel filtration.** Soluble venom (150 mg of protein) from *P. imperator* was loaded onto a Sephadex G-50 column (0.9 × 190 cm) and eluted with 20 mM ammonium acetate buffer, pH 4.7. Tubes containing 2.5-ml volume each were collected and pooled into five subfractions (*I–V*), according to the absorbance at 280 nm, as indicated by the *horizontal bars*. The active fraction V corresponds to ~38% of soluble venom.

tional experiments in the presence of valinomycin and found that fraction V still inhibited Ca^{2+} plateau levels even in the presence of this hyperpolarizing agent (data not shown, but data for purified toxin shown later).

Fraction V was further fractionated by running samples on a reverse-phase HPLC column and eluting samples with increasing strengths of acetonitrile as described under "Experimental Procedures." At least 35 distinct components were resolved by this chromatographic step (Fig. 4) that were collected as 13 individual subfractions for bioassay. Inhibition of the thapsigargin-stimulated Ca^{2+} plateau phase was observed only with subfraction 7 (Fig. 4, *asterisk*). Effects of three dilutions of subfraction 7 (*SF7*) are shown in Fig. 5 where increasing doses of subfraction 7 produced more extensive reduction of the Ca^{2+} plateau phase.

Subfraction 7 was then submitted to automatic Edman degradation, giving the amino acid sequence Leu-Trp-*X*-*X* where *X* was a mixture of amino acids (Lys, Ser, Gly, and Thr). This was an indication of the presence of more than one peptide in this subfraction 7. For this reason another chromatographic separation was conducted (see Fig. 4, *inset*), allowing the separation of two peptides for which the sequence was confirmed by post-source decay experiments using a MALDI-TOF mass spectrometer. Two distinct sequences were finally obtained. Peptide 1 eluting at 23.27 min had the amino acid sequence Leu-Trp-Ser-Gly with a molecular mass of 461.5 atomic mass units, and peptide 2 eluting at 23.82 min had the amino acid sequence Leu-Trp-Lys-Thr with a molecular mass of 546.6 atomic mass units. These short peptides are in small abundance in the venom. Peptide 1 is ~0.30%, whereas peptide 2 is only 0.17% of the total soluble venom. Significant amounts of peptide analogues containing *N*-formylkynurenine, an amino acid derivative resulting from Trp oxidation, were also detected in each fraction.

Since the amount of native peptides purified from the venom was too low for an extensive biological characterization and because we knew the amino acid sequences of the peptide toxins, we decided to synthesize both peptides. Approximately 30 mg were obtained for each peptide toxin. They were further separated by HPLC (data not shown) giving a yield of 60% for peptide 1 and 72% for peptide 2. The correct amino acid sequence of the synthetic peptides was confirmed by MS/MS analysis using the ion trap spectrometer as described under "Experimental Procedures." The effects of the synthetic peptides were investigated on SOCE.

Initial studies demonstrated that both peptides had inhibitory activities in terms of reducing the thapsigargin-stimulated Ca^{2+} plateau phase (data not shown). However, the potency of the peptides seemed to be somewhat low. Data for inhibition by peptide 2 showed that a dose of 1 μM was required to see measurable inhibition, and maximum inhibition was not observed until a dose of 20 μM was reached (Fig. 6*A*). Since subfraction 7 from the HPLC separation yielded two small peptides, we explored the possibility that these peptides might be associated into a complex that was responsible for the inhibitory activity in the *P. imperator* venom. We mixed peptide 1 and peptide 2 in a tube and submitted them to constant rotation for various periods of time ranging from hours to days and then tested the potency of the mixture at various time periods. We found that after 2 days of constant rotation a substantially lower dose of peptide was required for inhibition of SOCE. However, this observation was not unique to the mixture of peptide 1 and peptide 2 as we found that placing either peptide 1 alone or peptide 2 alone under similar conditions resulted in a substantial increase in their potency. The data in Fig. 6*B* show a representative dose response for peptide 2 treated under such conditions. With this material, one can observe a slight inhibitory effect at a peptide dose as low as 1 nM and a maximum effect at a peptide dose of 1 μM. At this maximum dose the Ca^{2+} plateau is reduced by ~50%.

To confirm that the modified peptide is inhibiting Ca^{2+} entry and not stimulating Ca^{2+} pumps, its effect on Ba^{2+} entry was measured. For this experiment, we incubated the cells in HBSS and then switched to a Ba^{2+}-containing, Ca^{2+}-free medium to obtain a brief measure of Ba^{2+} leak flux. The cells were then switched to 0 Ca^{2+} medium followed by 0 Ca^{2+} with 1 μM thapsigargin to deplete internal stores. Following the return of Ca^{2+} to basal levels, 2 mM Ba^{2+} was again added to monitor total Ba^{2+} entry. The SOCE was determined by subtracting the Ba^{2+} leak from the total Ba^{2+} entry. As is shown in Fig. 7*A*, the peptide at a dose of 1 μM inhibited Ba^{2+} entry by ~50%. A statistical analysis of a series of experiments at a peptide toxin concentration of 1 μM is shown (Fig. 7*B*). The slope of Ba^{2+} entry in the control was $0.00072 \pm 0.00004\ s^{-1}$ ($n = 13$), and in the presence of modified peptide toxin 2 (1 μM) it was $0.00038 \pm 0.00002\ s^{-1}$ ($n = 11$). These values are significantly different ($p = 0.00005$). To determine whether the peptide toxin was having its inhibitory effect by depolarizing the cells and thereby decreasing the driving force for Ca^{2+} entry, we ran similar experiments in the presence of valinomycin, which locks the membrane potential in a hyperpolarized state. We found that the addition of valinomycin slightly increased the thapsigargin-stimulated Ba^{2+} entry, consistent with the predicted effect of membrane hyperpolarization. However, in the presence of valinomycin the modified synthetic peptide 2 still inhibited SOCE by a comparable percentage (Fig. 8). In the presence of valinomycin, Ba^{2+} entry increased to $0.00084 \pm 0.00001\ s^{-1}$ ($n = 4$); the addition of modified peptide toxin 2 (1 μM) in the presence of valinomycin reduced Ba^{2+} entry to $0.00046 \pm 0.00006\ s^{-1}$ ($n = 4$). The difference in these values is statistically significant ($p = 0.03$).

To determine the specificity of the peptide toxin, we investigated its effect on another type of Ca^{2+} entry in HEK-293 cells. We determined the effect of the peptide toxin on Ca^{2+} entry stimulated by OAG. While in our previous studies (34) both TRPC1 and TRPC3 appear to mediate SOCE, in later studies we observed that only TRPC3 mediates OAG-stimulated Ca^{2+} entry (35). Following addition of 1 μM modified peptide toxin 2 to cells stimulated with OAG, no effect on the stimulated Ca^{2+} entry was observed (Fig. 9). Thus, the peptide toxin appears to be highly specific for Ca^{2+} entry activated by Ca^{2+} store depletion.

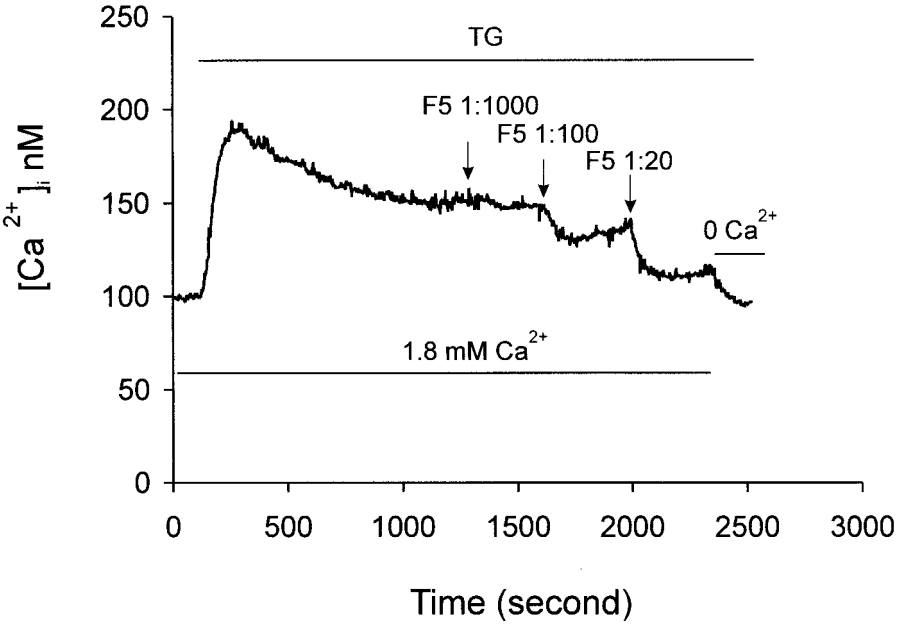

FIG. 3. **Inhibition of thapsigargin-stimulated Ca^{2+} entry by a partially purified fraction of the *P. imperator* venom.** Fraction V collected from the gel filtration column was diluted in HBSS, and its effect on thapsigargin (*TG*)-stimulated Ca^{2+} entry was determined. As described in Fig. 1, once the stable calcium plateau was established, different dilutions of the fraction V (*F5*) were added, and its effect on the Ca^{2+} plateau was monitored as a measurement of its effect on Ca^{2+} entry.

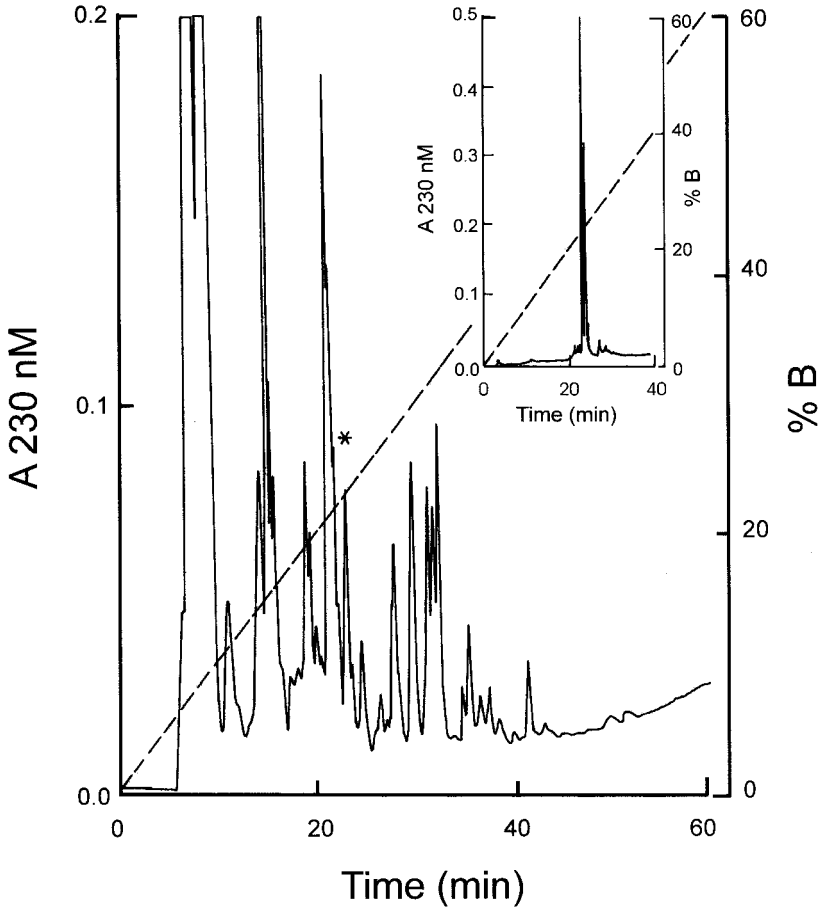

FIG. 4. **HPLC separation of fraction V of the *P. imperator* venom.** A 1.0-mg sample of fraction V protein from the Sephadex G-50 column was applied to a semipreparative C18 reverse-phase column, eluted with a linear gradient from solution A (0.12% trifluoroacetic acid in water) to 60% solution B (0.10% trifluoroacetic acid in acetonitrile), and run for 60 min. The active fraction (labeled with an *asterisk*) was further separated on an analytical C18 reverse-phase column eluted with the same gradient; its profile is shown in the *inset* of the figure (note that only the first section of the gradient is shown). Two pure peptides were obtained from this column and were further characterized.

As mentioned in the Introduction, 2-APB not only inhibits SOCE but also inhibits release of Ca^{2+} from internal stores. Thus, the question arose as to whether tetrapandins would also inhibit Ca^{2+} release from intracellular stores. To investigate this question, we monitored either thapsigargin-stimulated or CCh-stimulated Ca^{2+} release from intracellular stores. Control cells were incubated for 30 min in HBSS and washed quickly in Ca^{2+}-free HBSS, and then thapsigargin was added in a Ca^{2+}-free HBSS medium to release Ca^{2+} from intracellular stores. In parallel, cells were preincubated for 30 min in HBSS containing either 100 μM 2-APB or 1 μM tetrapandin 2 (both represent maximum doses for inhibition of Ca^{2+} entry) and washed quickly in Ca^{2+}-free HBSS, and then thapsigargin was added in Ca^{2+}-free HBBS in the continued presence of the inhibitors. As can be seen in Fig. 10*A*, the thapsigargin-induced release of Ca^{2+} was not modified by preincubation with tetrapandin 2 (*right panel*), while preincubation of cells with 2-APB blocked a substantial amount of the Ca^{2+} release (*center panel*). The

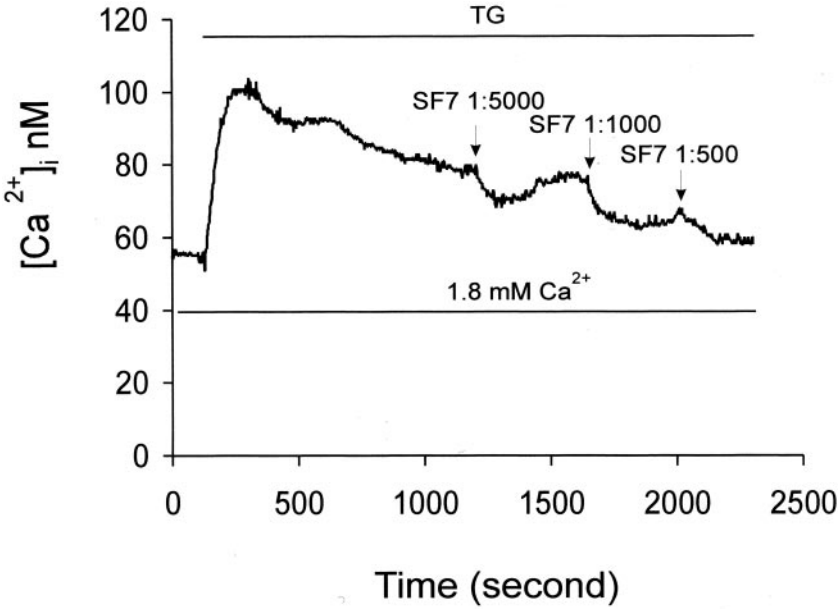

FIG. 5. **Inhibition of thapsigargin-stimulated Ca^{2+} entry by an HPLC-purified subfraction of the *P. imperator* venom.** Fraction V from the G-50 filtration column was further fractionated by reverse-phase HPLC, and the eluted subfraction 7 was diluted in HBSS for fura-2 imaging experiments. As described in Fig. 1, once the stable calcium plateau was established, different dilutions of the subfraction 7 (*SF7*) were added, and its effect on the Ca^{2+} plateau phase was monitored as a measurement of its effect on Ca^{2+} entry. *TG*, thapsigargin.

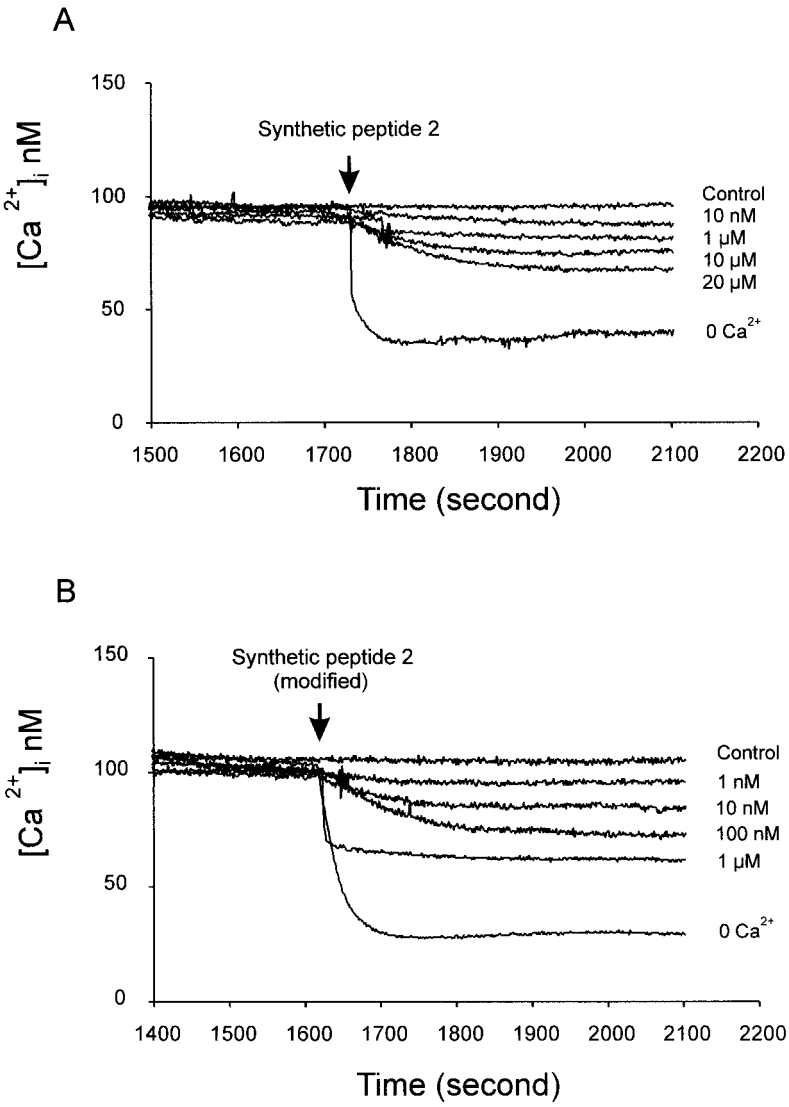

FIG. 6. **Dose response for inhibition of thapsigargin-stimulated Ca^{2+} entry by synthetic toxin peptide.** The synthetic toxin peptide 2 was dissolved in HBSS, and a portion of the solution was utilized directly for imaging experiments (*A*). Another portion of the toxin solution was filter-sterilized, and the solution was rotated on a Glas-Col rotator for 2 days at room temperature before utilization in fura-2 imaging experiments (*B*). HEK-293 cells were stimulated with thapsigargin (1 μM) in HBSS, and after the calcium plateau was achieved, the synthetic peptide was added at the concentrations of 10 nM, 1 μM, 10 μM, and 20 μM (*A*), or the modified synthetic peptide was added at the concentrations of 1 nM, 10 nM, 100 nM, and 1 μM (*B*). The effect on the thapsigargin-induced Ca^{2+} plateau was monitored as a measurement of the toxin effect on Ca^{2+} entry.

average peak height for the thapsigargin control was 143 ± 5.8 nM (n = 8) compared with 143 ± 13.9 nM (n = 8) for tetrapandin 2-treated cells or 84.3 ± 9.9 nM (n = 10, statistically different from control, $p < 0.0002$) for 2-APB-treated cells. Similarly, if CCh was utilized to release Ca^{2+} from $InsP_3$-sensitive stores (Fig. 10*B*), tetrapandin 2 had no effect on the Ca^{2+} release

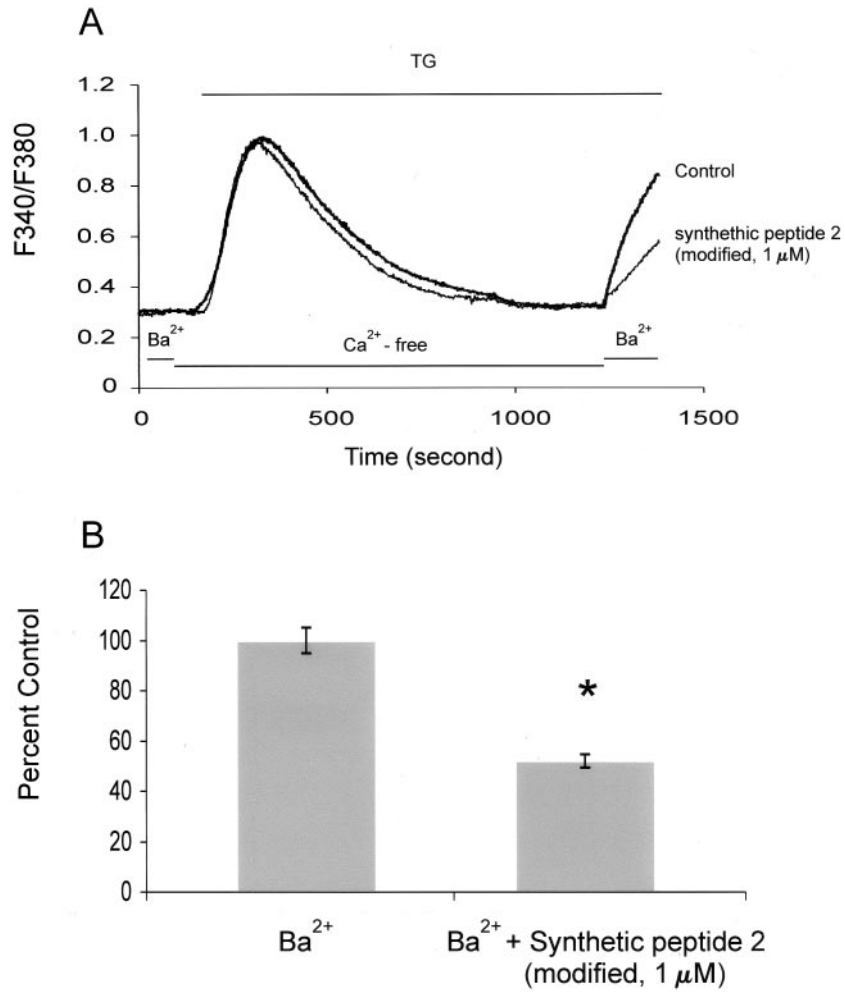

FIG. 7. **Inhibition of thapsigargin-stimulated Ba^{2+} entry by modified synthetic toxin peptide.** *A*, HEK-293 cells were incubated in HBSS to establish a base line prior to switching into Ca^{2+}-free HBSS. A Ca^{2+}-free, 2 mM Ba^{2+} HBSS solution was added briefly to the cells to measure the Ba^{2+} leak. Following a return to Ca^{2+}-free HBSS, cells were stimulated with thapsigargin (*TG*, 1 μM), and after cytosolic Ca^{2+} returned to basal levels, 2 mM Ba^{2+} was added. SOCE was defined as the leak-subtracted, TG-stimulated Ba^{2+} influx. In half of the coverslips, the modified synthetic peptide 2 (1 μM) was mixed with 2 mM Ba^{2+} solution, and it was applied after thapsigargin depletion of Ca^{2+} stores (*thin line*). The results obtained were compared with the control (*thick line*) for which a comparable amount of vehicle was added. *B*, the Ba^{2+} entry values were plotted as percentage of control. At a dose of 1 μM modified peptide toxin 2, SOCE was reduced by 48 ± 2%. *, significantly different from control ($p < 0.0001$).

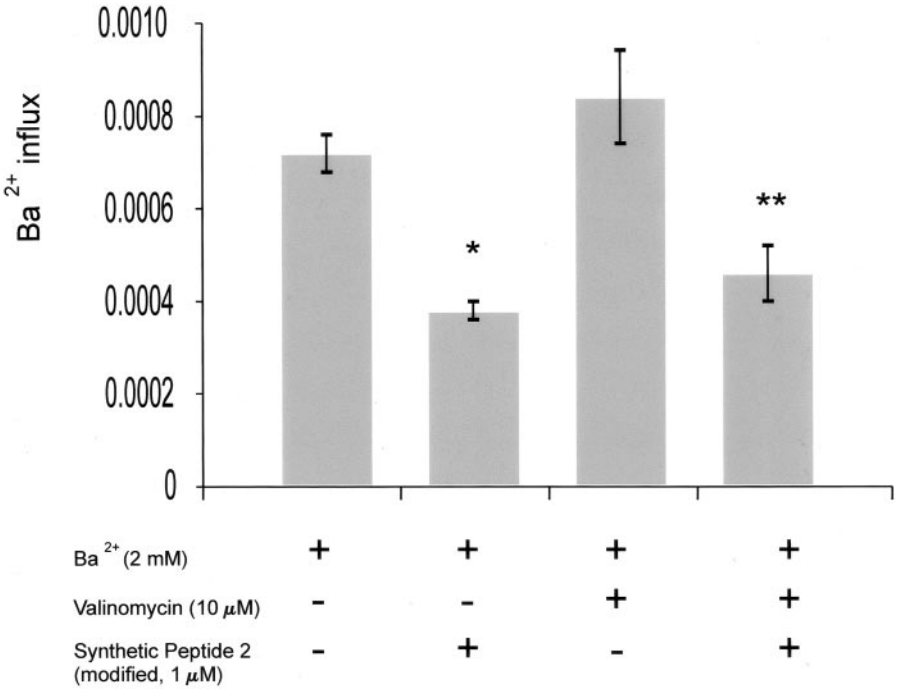

FIG. 8. **Effect of valinomycin on inhibition of SOCE by modified synthetic toxin peptide.** Ba^{2+} entry experiments similar to those described in Fig. 7 were performed in the presence of 10 μM valinomycin. Statistical analysis of the data with the mean value of the leak-subtracted Ba^{2+} entry representing the amount of SOCE is shown. *, significantly different from control ($p < 0.0001$). **, significantly different from valinomycin alone ($p < 0.03$).

(*right panel*), while 2-APB had a substantial inhibitory effect (*center panel*). The average peak height for the CCh control was 245.6 ± 26.7 nM ($n = 5$) compared with 276.8 ± 18.8 nM ($n = 4$) for the CCh response in cells preincubated with tetrapandin 2 or 53.2 ± 7.9 nM ($n = 9$) for cells preincubated with 2-APB.

We also wanted to compare the effect of tetrapandins to that of 2-APB on the plateau phase of the CCh-stimulated Ca^{2+}

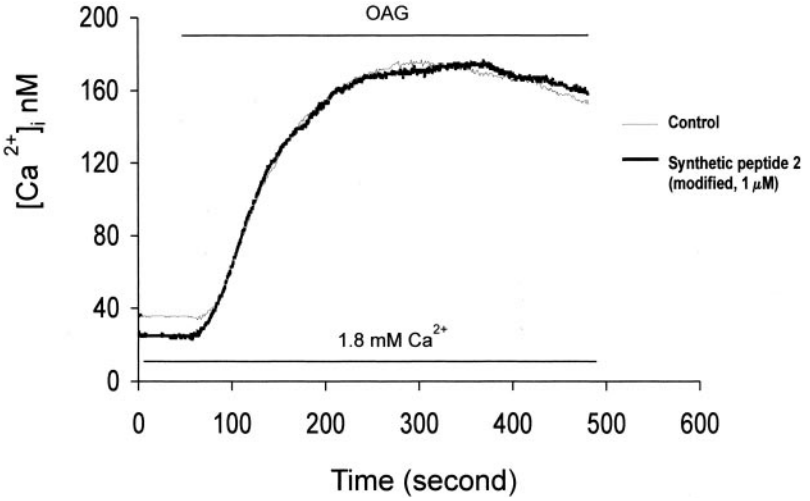

FIG. 9. **Effect of synthetic toxin peptide on OAG-induced Ca^{2+} entry.** HEK-293 cells were stimulated with 100 μM OAG. The OAG-induced Ca^{2+} entry was measured in the presence (*thick line*) or in the absence (*thin line*) of the modified synthetic peptide toxin 2 (1 μM). The data are representative of nine separate measurements.

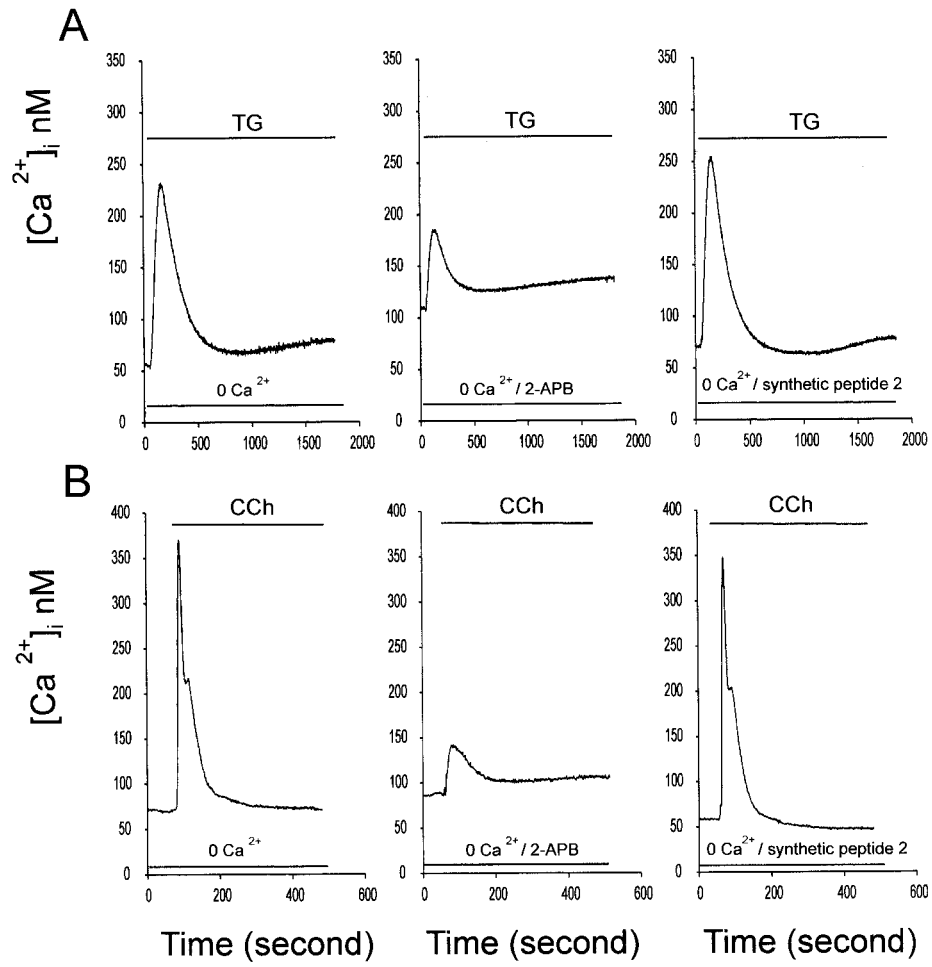

FIG. 10. **Effect of synthetic toxin peptide on thapsigargin- or CCh-induced intracellular Ca^{2+} release.** HEK-293 cells were preincubated for 30 min in HBSS with either no addition (*left panel*), 100 μM 2-APB (*middle panel*), or 1 μM modified synthetic peptide 2 (*right panel*). The preincubation period was followed by a 1-min incubation in Ca^{2+}-free HBSS before addition of either 1 μM thapsigargin (*TG*) (*A*) or 100 μM CCh (*B*) to release Ca^{2+} from intracellular stores. Inhibitors were present throughout the Ca^{2+} release phase. Each trace represents an averaged response from at least 800 cells on a single coverslip.

response. Cells were treated with 100 μM CCh in HBSS and allowed to establish a stable plateau phase. In control cells, the HBSS was replaced with Ca^{2+}-free HBSS to establish that the plateau phase is dependent on a continued influx of Ca^{2+} (Fig. 11*A*). For the 2-APB and tetrapandin conditions, these drugs were added during the plateau phase in the continued presence of HBSS. The data in Fig. 11*B* show that addition of 2-APB resulted in a substantial reduction of the plateau Ca^{2+} level. A similar response was observed with the addition of tetrapandin 2 (Fig. 11*C*). The removal of Ca^{2+} from the external medium brought the Ca^{2+} value 97 ± 1.3% (n = 5) of the way back down to basal levels. In comparison, 2-APB brought the Ca^{2+} value 76 ± 3.3% (n = 6) of the way back down to basal levels, while tetrapandin 2 brought the Ca^{2+} value 70.4 ± 5.0% (n = 9) of the way back down to basal levels.

DISCUSSION

In this study, we found an inhibitory effect on SOCE by venom from the African scorpion *P. imperator*. This inhibitory activity appears to be uncommon among venoms from snakes and other scorpions as we found it in only one of 14 snake venoms and in one of four scorpion venoms tested. This finding encouraged us to proceed since it indicated that we were not observing a nonspecific effect of venoms in general, such as

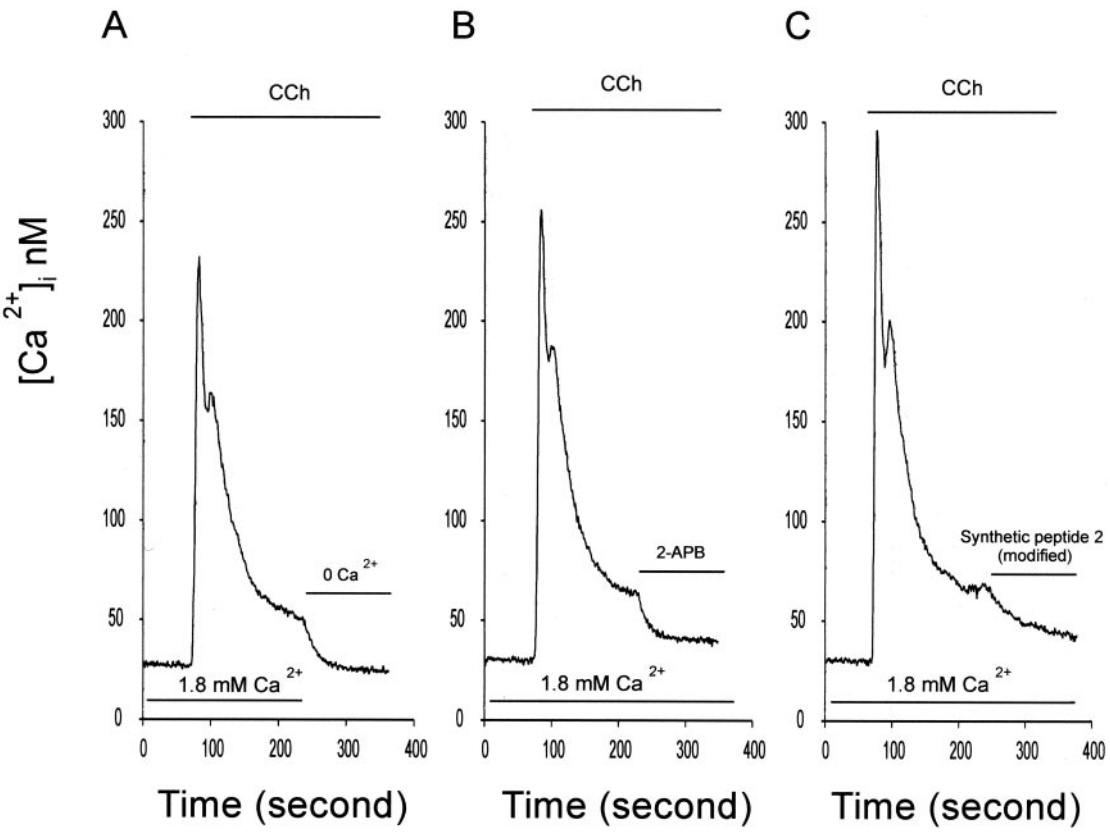

FIG. 11. **Effect of synthetic toxin peptide on the plateau phase of the CCh-induced Ca^{2+} response.** HEK-293 cells in HBSS were stimulated with 100 μM CCh. Once a stable plateau phase was established, the HBSS solution was replaced with either Ca^{2+}-free HBSS (*A*), HBSS containing 100 μM 2-APB (*B*), or HBSS containing 1 μM modified synthetic peptide 2 (*C*). Each trace represents the averaged response from at least 800 cells on a single coverslip.

membrane depolarization due to toxin action on other ion channels. This was further supported by the finding that the venom still inhibited thapsigargin-stimulated Ca^{2+} entry even in the presence of valinomycin, which locks the membrane potential in a hyperpolarized state.

We have outlined the steps involved in the purification of a peptide toxin from the *P. imperator* venom as well those involved in the sequencing and chemical synthesis of a peptide toxin that inhibits SOCE. Two short peptides were found to be present in the HPLC subfraction 7. Both peptides were tetrapeptides (LWSG and LWKT) and were found to share two amino acids in common.

These peptide toxins were named tetrapandins 1 and 2 (peptides 1 and 2, respectively) from the fact that they come from the scorpion of the genus *Pandinus* and have only four amino acids. This is quite unique among the venom components isolated and characterized thus far in the literature. Most scorpion venoms contain peptides that modify or block the function of ion channels such as voltage-dependent K^+ and Na^+ channels, although other venoms also have peptides capable of impairing the function of Cl^- channels or Ca^{2+}-sensitive ryanodine channels (for a review, see Ref. 36). Actually, from the venom of the same *P. imperator*, several interesting peptides were isolated previously, such as imperatoxin a and b (for a review, see Ref. 37) and scorpine, a defensin and antimalaria agent (38). The findings described here should not be taken as unusual since of the 100,000 components estimated to exist in scorpion venoms alone, only over 300 components have been studied thus far (36, 39, 40). Most of the studies reported in the literature deal with peptides from 26 to 76 amino acid residues long, but very few, if any, studies have been performed with the low molecular weight components of these venoms, which elute from the Sephadex G-50 column in fraction V.

Tetrapandins 1 and 2 have a lipophilic segment as well as a hydrophilic segment. The side chains of Leu and Trp are hydrophobic, whereas the C-terminal carboxylic groups and side chains of Lys and hydroxyl groups of Ser and Thr are hydrophilic. Since these peptides have a hydrophobic segment and knowing that biological membranes are permeable to hydrophobic substances, it is possible that these peptides might cross the cell membrane. This would provide the possibility that their effect could be at either an external or internal channel site to inhibit SOCE.

Both synthetic peptides have inhibitory action on SOCE when they are freshly prepared, although their potency is somewhat low. However, upon continued rotation for 2 days both peptides greatly increase their potency for inhibition of SOCE. After modification, the peptide toxins can initiate their effects at a dose of 1 nM, which is considerably lower than the 1 μM dose required for a threshold effect to be seen with freshly prepared toxin. At present, we are not sure whether the peptides are chemically modified (*e.g.* air-oxidized) to a new structure or whether they aggregate during the incubation period. It is tempting to speculate that Trp oxidation to *N*-formylkynurenine might be responsible for such an increase in biological activity since a significant amount of the peptide purified from *P. imperator* venom showed signs of Trp oxidation. On the other hand, since they are amphiphilic substances (partially hydrophilic and hydrophobic) some kind of aggregation (dimerization or micelle formation) could occur with these peptides that could be responsible for the increased activity seen after agitation at room temperature. Thus, while a number of experiments are still needed to elucidate the exact modification of the synthetic peptides required to obtain the highest potency, we have clearly obtained a preparation that should be quite useful for the further exploration of SOCs.

One interesting aspect of this peptide toxin is that at a maximum dose it inhibits only 50% of either the thapsigargin-stimulated Ca^{2+} plateau phase or the thapsigargin-stimulated Ba^{2+} entry. This is in direct contrast to the effects of 2-APB, which has been shown to inhibit ~90% of the thapsigargin-stimulated Ba^{2+} entry in these cells (35). However, 2-APB also is known to inhibit release of Ca^{2+} from internal stores. Our data indicate that the tetrapandins are more specific than 2-APB in that they have no effect on release of internal Ca^{2+} stores under conditions where 2-APB dramatically reduces Ca^{2+} store release. This is true whether the store Ca^{2+} is released by thapsigargin or by $InsP_3$ production in response to CCh stimulation (Fig. 10).

The 50% maximal reduction of thapsigargin-stimulated Ca^{2+} entry may suggest either a partial block of SOCs or full inhibition of one of multiple Ca^{2+} entry pathways activated by thapsigargin. Previous studies have suggested that there may be more than one pathway activated in response to thapsigargin (8). For example, our previous TRPC3 antisense data (34) indicate that suppression of ~60% of the TRPC3 protein reduces SOCE by only 32%. Thus, extrapolation of this data to full TRPC3 protein suppression suggests that TRPC3 may mediate at most 45–50% of the total SOCE. Thus, it is possible that the toxin may be inhibiting in a selective manner either the TRPC3-sensitive or the TRPC3-insensitive portion of the thapsigargin-stimulated Ca^{2+} entry. We are currently using small interfering RNA technology to try to achieve a more efficient reduction of TRPC3 levels in HEK-293 cells. If we can suppress TRPC3 levels by ~90%, then we will be in a better position to address the question of whether tetrapandins are working on the TRPC3-sensitive or TRPC3-insensitive pathway. The alternative possibility, that the toxin is partially blocking the store-operated channel, can be best tested by electrophysiological methods. Electrophysiological experiments to characterize the mechanism for inhibition of SOCE by tetrapandins will be performed in the near future. However, it is also possible for the tetrapandins to work via a mechanism other than direct interaction with the channel pore. There is much evidence for a conformational coupling mechanism for activating SOCs whereby direct interaction between TRPC3 channels and $InsP_3$ receptors is important. Given the potential for a small peptide with a hydrophobic segment to penetrate the plasma membrane, it is possible that tetrapandins penetrate the plasma membrane and perturb the coupling between TRPC3 channels and $InsP_3$ receptors. If the small interfering RNA experiments demonstrate that it is the TRPC3-dependent pathway that is inhibited by tetrapandins, this possibility will be explored in depth.

In regard to the potential use of tetrapandins to explore various Ca^{2+} entry pathways, it was observed that tetrapandins were ineffective in blocking the Ca^{2+} entry stimulated by OAG (Fig. 9) yet were fairly effective in blocking the CCh-stimulated Ca^{2+} plateau phase (Fig. 11). Thus, tetrapandins may be useful in resolving the question of the involvement of SOCs (or subtypes of SOCs) and OAG-stimulated channels in the Ca^{2+} response stimulated by CCh or other G protein-coupled receptor agonists. On another level, the tetrapandins should be extremely valuable in establishing which downstream physiological responses are regulated by SOCE.

Acknowledgments—The assistance of Dr. Cesar V. F. Batista on MS analysis, biologist Cipriano Balderas in milking the scorpions, and Grzegorz Gurda in some preliminary imaging experiments is greatly acknowledged. We also thank the Kentucky Reptile Zoo (Slade, KY) and its director Jim Harrison for providing the snake venoms for our investigation.

REFERENCES

1. Fasolato, C., Innocenti, B., and Pozzan, T. (1994) *Trends Pharmacol. Sci.* **15,** 77–83
2. Barritt, G. J. (1999) *Biochem. J.* **337,** 153–169
3. Parekh, A. B., and Penner, R. (1997) *Physiol. Rev.* **77,** 901–930
4. Bootman, M. D., Berridge, M. J., and Roderick, H. L. (2002) *Curr. Biol.* **12,** R563–565
5. Putney, J. W., Jr. (1986) *Cell Calcium* **7,** 1–12
6. Putney, J. W., Jr., Broad, L. M., Braun, F. J., Lievremont, J. P., and Bird, G. S. (2001) *J. Cell Sci.* **114,** 2223–2229
7. Zitt, C., Halaszovich, C. R., and Luckhoff, A. (2002) *Prog. Neurobiol.* **66,** 243–264
8. Dietl, P., Haller, T., Wirleitner, B., and Friedrich, F. (1996) *Cell Calcium* **20,** 11–19
9. Jenkins, R. E., Hawley, S. R., Promwikorn, W., Brown, J., Hamlett, J., and Pennington, S. R. (2001) *Proteomics* **1,** 1092–1104
10. Hong, S. J., Lin, W. W., and Chang, C. C. (1994) *J. Biomed. Sci.* **1,** 172–178
11. Schwarz, G., Droogmans, G., and Nilius, B. (1994) *Cell Calcium* **15,** 45–54
12. de la Rosa, L. A., Alfonso, A., Vilarino, N., Vieytes, M. R., Yasumoto, T., and Botana, L. M. (2001) *Cell. Signal.* **13,** 711–716
13. Soergel, D. G., Yasumoto, T., Daly, J. W., and Gusovsky, F. (1992) *Mol. Pharmacol.* **41,** 487–493
14. Hong, S. J., and Chang, C. C. (1994) *Eur. J. Pharmacol.* **265,** 35–42
15. Alessandro, R., Masiero, L., Liotta, L. A., and Kohn, E. C. (1996) *In Vivo* **10,** 153–160
16. Bootman, M. D., Collins, T. J., Mackenzie, L., Roderick, H. L., Berridge, M. J., and Peppiatt, C. M. (2002) *FASEB J.* **16,** 1145–1150
17. Hupe, D. J., Boltz, R., Cohen, C. J., Felix, J., Ham, E., Miller, D., Soderman, D., and Van Skiver, D. (1991) *J. Biol. Chem.* **266,** 10136–10142
18. Luo, D., Broad, L. M., Bird, G. S., and Putney, J. W., Jr. (2001) *J. Biol. Chem.* **276,** 5613–5621
19. Ma, H. T., Patterson, R. L., van Rossum, D. B., Birnbaumer, L., Mikoshiba, K., and Gill, D. L. (2000) *Science* **287,** 1647–1651
20. Peppiatt, C. M., Collins, T. J., Mackenzie, L., Conway, S. J., Holmes, A. B., Bootman, M. D., Berridge, M. J., Seo, J. T., and Roderick, H. L. (2003) *Cell Calcium* **34,** 97–108
21. Wang, Y., Deshpande, M., and Payne, R. (2002) *Cell Calcium* **32,** 209–216
22. Bilmen, J. G., Wootton, L. L., Godfrey, R. E., Smart, O. S., and Michelangeli, F. (2002) *Eur. J. Biochem.* **269,** 3678–3687
23. Harks, E. G., Camina, J. P., Peters, P. H., Ypey, D. L., Scheenen, W. J., van Zoelen, E. J., and Theuvenet, A. P. (2003) *FASEB J.* **17,** 941–943
24. Chinopoulos, C., Starkov, A. A., and Fiskum, G. (2003) *J. Biol. Chem.* **278,** 27382–27389
25. Braun, F. J., Aziz, O., and Putney, J. W., Jr. (2003) *Mol. Pharmacol.* **63,** 1304–1311
26. Kao, C. Y. (1966) *Pharmacol. Rev.* **18,** 997–1049
27. Carbone, E., Wanke, E., Prestipino, G., Possani, L. D., and Maelicke, A. (1982) *Nature* **296,** 90–91
28. Olivera, B. M., Imperial, J. S., Cruz, L. J., Bindokas, V. P., Venema, V. J., and Adams, M. E. (1991) *Ann. N. Y. Acad. Sci.* **635,** 114–122
29. Keith, R. A., Mangano, T. J., and Salama, A. I. (1989) *Br. J. Pharmacol.* **98,** 767–772
30. Zamudio, F. Z., Conde, R., Arevalo, C., Becerril, B., Martin, B. M., Valdivia, H. H., and Possani, L. D. (1997) *J. Biol. Chem.* **272,** 11886–11894
31. Merrifield, B. (1963) *J. Am. Chem. Soc.* **85,** 2144–2154
32. Schilling, W. P., Rajan, L., and Strobl-Jager, E. (1989) *J. Biol. Chem.* **264,** 12838–12848
33. Kwan, C. Y., and Putney, J. W., Jr. (1990) *J. Biol. Chem.* **265,** 678–684
34. Wu, X., Babnigg, G., and Villereal, M. L. (2000) *Am. J. Physiol.* **278,** C526–C536
35. Wu, X., Babnigg, G., Zagranichnaya, T., and Villereal, M. L. (2002) *J. Biol. Chem.* **277,** 13597–13608
36. Possani, L. D., Merino, E., Corona, M., Bolivar, F., and Becerril, B. (2000) *Biochimie (Paris)* **82,** 861–868
37. Valdivia, H. H., and Possani, L. D. (1998) *Trends Cardiovasc. Med.* **8,** 111–118
38. Conde, R., Zamudio, F. Z., Rodriguez, M. H., and Possani, L. D. (2000) *FEBS Lett.* **471,** 165–168
39. Possani, L. D., Becerril, B., Delepierre, M., and Tytgat, J. (1999) *Eur. J. Biochem.* **264,** 287–300
40. Possani, L. D., Selisko, B., and Gurrola, G. (1999) *Perspect. Drug Discov. Des.* **15/16,** 15–40

Tetrapandins, a New Class of Scorpion Toxins That Specifically Inhibit Store-operated Calcium Entry in Human Embryonic Kidney-293 Cells

Andree Shalabi, Fernando Zamudio, Xiaoyan Wu, Andrea Scaloni, Lourival D. Possani and Mitchel L. Villereal

J. Biol. Chem. 2004, 279:1040-1049.
doi: 10.1074/jbc.M308234200 originally published online October 28, 2003
